

# Measurement and mitigation of multiple reflection effects on the Differential Group Delay spectrum of optical components

P.A. Williams and J.D. Kofler

National Institute of Standards and Technology - Boulder, Colorado, USA

**Abstract:** *Ripple in the Differential Group Delay (DGD) spectrum due to multiple reflections is described theoretically and demonstrated experimentally. A technique of tilting the cavity element to reduce these multiple reflection effects is discussed and is demonstrated to remove the ripples in the DGD spectrum.*

## I. Introduction

In the field of optical fiber metrology, it seems that you can't measure anything without the result being affected by multiple reflections coming from a cavity somewhere in the optical path. Polarization-Mode Dispersion (PMD) or, more specifically, Differential Group Delay (DGD) is also affected by multiple reflections. The result is a ripple in the DGD spectrum with a surprisingly large amplitude [1].

In this paper, we derive the spectral DGD behavior in the presence of multiple reflections, and demonstrate how these effects can be significantly reduced by tilting the cavity component with respect to the optical path.

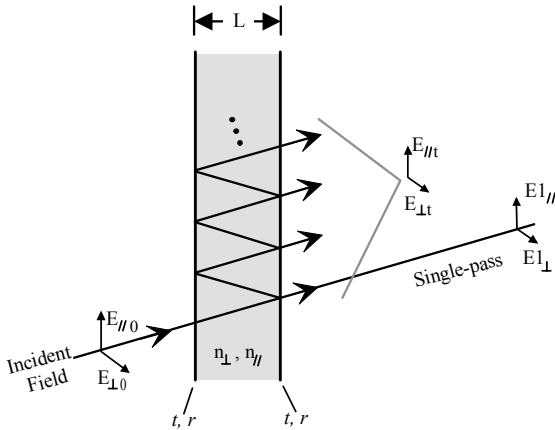


**Figure 1.** Schematic of Fabry-Perot cavity with transmission and reflection coefficients  $t$  and  $r$ , containing birefringent material with indices of refraction  $n_{//}$  and  $n_{\perp}$ .

## II. Theory

We derive the DGD spectrum of a cavity composed of a simple birefringent material whose eigenaxes are independent of wavelength ("non-

mode-coupled"). The physical length of the cavity is  $L$ , and its birefringence is  $\Delta n = (n_{//} - n_{\perp})$ . For simplicity, we assume the transmission and reflection coefficients ( $t$  and  $r$ ) at the input interface are equal to those at the output interface. Figure 1 illustrates the geometry. Note: this derivation assumes that the cavity is not tilted with respect to the light beam (ie. normal incidence). The tilted light beam in Figure 1 is only shown to schematically to illustrate the features.

We calculate the transmitted electric field for the two orthogonal polarization components aligned with the birefringence axes of the cavity. The electric field of the light that is transmitted through the cavity without experiencing any reflections ("single-pass") is given by

$$\begin{aligned} E_{//} &= E_{//0} e^{i\delta_{//} t^2}, \\ E_{\perp} &= E_{\perp0} e^{i\delta_{\perp} t^2}. \end{aligned} \quad (1)$$

$E_{//0}$  and  $E_{\perp0}$  are the input electric fields, and  $\delta_{//}$  and  $\delta_{\perp}$  are the phase delays accumulated by a single pass through the cavity for light polarized along each birefringent axis of the cavity. The phase delays are given as

$$\delta_a = \omega n_a L / c, \quad (2)$$

where  $\omega$  is the (radian) optical frequency,  $c$  is the speed of light,  $n$  is the index of refraction with the subscript  $a$  denoting the corresponding polarization state ( $//$  or  $\perp$ ).

Group delay is given by the radian-frequency derivative of transmitted phase. So, we can find the DGD of the single-pass transmission as the difference in group delay for the two orthogonal components,

$$\frac{d(\delta_{//} - \delta_{\perp})}{d\omega} = \left( \Delta n + \omega \frac{d\Delta n}{d\omega} \right) \frac{L}{c} = \frac{\Delta n_g L}{c}, \quad (3)$$

where  $\Delta n$  is the phase birefringence and  $\Delta n_g = n_{//,g} - n_{\perp,g}$  is the group birefringence, with

$$n_{a,g} = n_a + \omega \frac{dn_a}{d\omega}. \quad (4)$$

So we find that the DGD seen by the single-pass light is

$$\Delta\tau_0 = \frac{\Delta n_g L}{c} = (n_{//,g} - n_{\perp,g}) \frac{L}{c}. \quad (5)$$

This is the DGD that would be measured in this device if there were no reflections.

In order to find how the DGD is modified by multiple reflections, we use a standard Fabry-Perot approach [2] to write the vector components of the total electric fields transmitted through the cavity as

$$E_{//t} = E_{//0} \left[ \frac{t^2}{1 - r^2 e^{-i2\delta_{//}}} \right], \quad (6)$$

and

$$E_{\perp t} = E_{\perp 0} \left[ \frac{t^2}{1 - r^2 e^{-i2\delta_{\perp}}} \right], \quad (7)$$

where a term containing the time dependence is common to both and omitted. The phases of  $E_{//t}$  and  $E_{\perp t}$  do not include the phase accumulated by the first pass through the device. In other words, the phase in Equations (6) and (7) is the perturbation to the transmitted phase caused by multiple reflections.

Writing the expressions for  $E_{//t}$  and  $E_{\perp t}$  in phasor notation, we find the phases of each component:

$$\varphi_{//} = \tan^{-1} \left( \frac{-R \sin 2\delta_{//}}{1 - R \cos 2\delta_{//}} \right), \quad (8)$$

and

$$\varphi_{\perp} = \tan^{-1} \left( \frac{-R \sin 2\delta_{\perp}}{1 - R \cos 2\delta_{\perp}} \right), \quad (9)$$

where  $R$ , the intensity reflection coefficient, has been substituted for  $r^2$ .

We find the perturbation to the DGD caused by multiple reflections as

$$\Delta\tau_{FR} = \frac{d(\varphi_{//} - \varphi_{\perp})}{d\omega}, \quad (10)$$

or

$$\Delta\tau_{FR} = \frac{-2LR(\cos 2\delta_{//} - R)n_{//,g}}{(1 + R^2 - 2R \cos 2\delta_{//})c} + \frac{2LR(\cos 2\delta_{\perp} - R)n_{\perp,g}}{(1 + R^2 - 2R \cos 2\delta_{\perp})c}. \quad (11)$$

Since the complicated nature of Equation (11) clouds intuition about its behavior, we approximate  $\Delta\tau_{FR}$  as

$$\Delta\tau_{FR} \approx 4R\tau_0 \sin\left(\frac{2\omega n L}{c}\right) \sin\left(\frac{\omega \Delta n L}{c}\right), \quad (12)$$

where

$$\tau_0 = n_g L / c \quad (13)$$

is the group delay for a single-pass through the cavity. Equation (12) requires the assumptions  $R < 0.1$ , and  $\Delta\tau_0 / \tau_0 < 1$ .

The total DGD measured for transmission through the Fabry-Perot cavity of Figure 1 is the sum of the single-pass DGD plus the perturbation DGD

$$\Delta\tau = \Delta\tau_0 + \Delta\tau_{FR}. \quad (14)$$

Equations (11) and (12) predict some important features of the perturbation to the DGD spectrum. Equation (11) has two obvious periodicities due to the  $\cos(2\delta_{//})$  and  $\cos(2\delta_{\perp})$  terms. Since  $\delta_{//}$  and  $\delta_{\perp}$  are functions of  $\omega$ , we expect the first term of Equation (11) to repeat over a frequency spacing or Free Spectral Range (FSR) of

$$\Delta\omega_{//} = \frac{\pi c}{L n_{//,g}}. \quad (15)$$

Likewise, the second term repeats over a FSR

$$\Delta\omega_{\perp} = \frac{\pi c}{L n_{\perp,g}}. \quad (16)$$

Note that the refractive indices in Equations (15) and (16) are group (rather than phase) due to the frequency dependence of  $n$ . When combined, these two ripple ‘‘periods’’ will result in a fast ripple on  $\Delta\tau_{FR}$  that repeats over a frequency spacing of

$$\Delta\omega_0 = \left( \frac{1}{2\Delta\omega_{//}} + \frac{1}{2\Delta\omega_{\perp}} \right)^{-1} = \frac{\pi c}{L n_g}, \quad (17)$$

and in a ‘‘beat note’’ in the spectrum with a frequency spacing of

$$\Delta\omega_B = \left( \frac{1}{\Delta\omega_{//}} - \frac{1}{\Delta\omega_{\perp}} \right)^{-1} = \frac{\pi c}{L \Delta n_g}. \quad (18)$$

This behavior is more obvious in Equation (12) where the sine function at the left gives the fast ripples and the one at the right gives the envelope. Plots of the spectral behavior of Equation

(11) are shown Figures 2 and 3. The parameters used to generate these plots were:  $L = 9.97$  mm,  $R = 0.0014$ ,  $n = 1.532$ ,  $\Delta n = 0.00847$ ,  $n_g = 1.554$ , and  $\Delta n_g = 0.0094$ . These values were chosen to emulate the pigtailed quartz plate we measure in Section III.

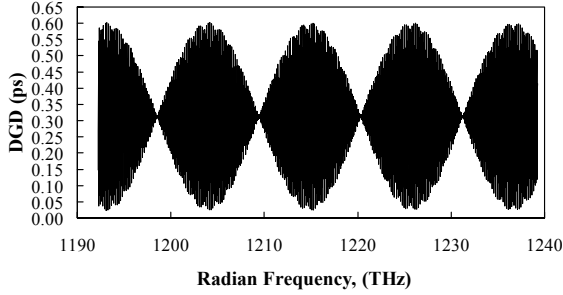


**Figure 2.** Simulated DGD spectrum showing Frequency beat notes due to multiple reflections in a birefringent cavity (from Equations (5), (11), and (14)).

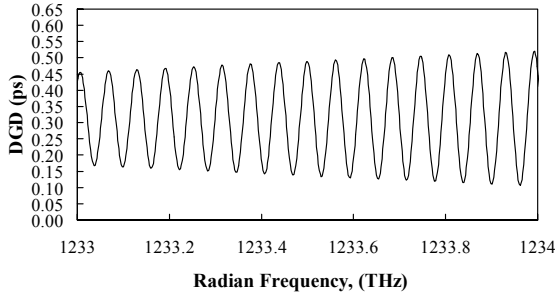


**Figure 3.** Close-up of DGD spectrum in Figure 2.

Equation (12) gives the amplitude of the ripple envelope as  $4R\tau_0$ . This result is somewhat surprising in that the ripple amplitude depends on the group delay of the cavity  $\tau_0$  and not the DGD  $\Delta\tau_0$ . Since typical sources of birefringence in components have  $\tau_0/\Delta\tau_0 \gg 1$ , the amplitude of the DGD spectral ripple can easily be larger than the DGD itself.

### III. Experimental Verification

These predictions are experimentally verified by measuring the DGD spectrum of a pigtailed quartz plate using a Modulation-Phase-Shift (MPS) technique [3] with a spectral resolution of  $\Delta\omega = 4.92$  GHz and a temporal resolution of 30 fs (yielding a bandwidth efficiency factor [4] of over 6700). The length and indices of refraction of the quartz plate are expected to be equal to those used in the above simulation. Both faces of the plate have a broadband anti-reflection coat-

ing expected to yield an  $R$  of 0.01-0.02, but this was not measured directly.

Figures 4 and 5 show the measured DGD spectrum for this device. We see qualitative agreement with the theoretical predictions of Figures 2 and 3 when an  $R$  of 0.0014 is used. This unexpectedly low  $R$  value was estimated by using  $R$  as a fitting parameter in Equation (12) to match the size of the ripple envelope in Figure 4. We attribute this low  $R$  value to a possible tilt of the waveplate, preventing some of the forward reflected light from being captured.

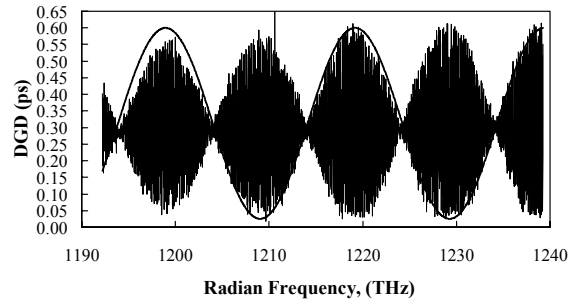


**Figure 4.** Measured DGD spectrum for pigtailed quartz plate with envelope portion of Equation (12) overlaid to estimate  $R$ .

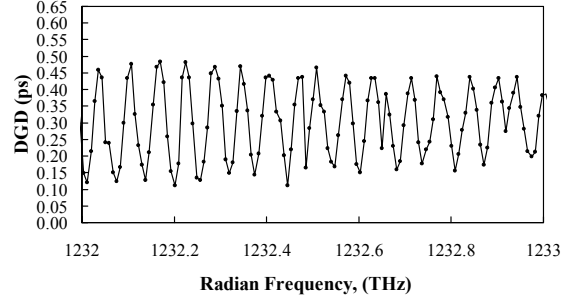


**Figure 5.** Close-up of DGD spectrum in Figure 4.

By counting cycles in Figures 4 and 5, we measured the frequency spacings  $\Delta\omega_0$  and  $\Delta\omega_B$  to be  $6.16 \times 10^{10} \text{ s}^{-1}$  and  $1.00 \times 10^{13} \text{ s}^{-1}$ , respectively. Inserting  $\Delta\omega_0$ ,  $\Delta\omega_B$  and our estimate of the quartz plate thickness  $L = 9.97$  mm into Equations (17) and (18) yields estimates for  $n_g$  and  $\Delta n_g$  of 1.53 and 0.0094 respectively. These predicted values are in good agreement (1.5 %) with the expected values of 1.554 and 0.0094.

### IV. Mitigation

An efficient means for reducing multiple reflections in the backward direction (return loss) is to

tilt the cavity element so that the backward-reflected beam reflects at an angle and misses the launch optics. However, in order to reduce the multiple reflection effect on DGD, we must suppress the multiple reflections that propagate in the forward direction. In general, this requires a larger tilt angle, since the forward-reflected beams experience only a transverse offset with tilt. Figure 6 illustrates how tilting the cavity lets the single-pass beam enter the collection optics, but causes a forward-reflected beam to miss.

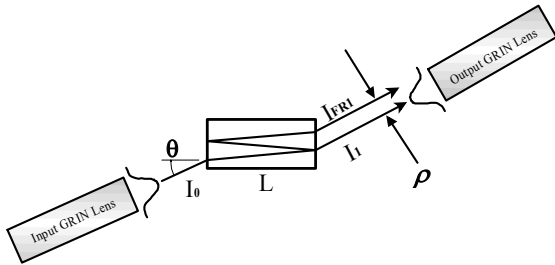


**Figure 6.** Schematic of launching light into tilted cavity element at angle  $\theta$  to prevent the reflected beams from being captured.

From Figure 6, we see that the transverse offset  $\rho$  between the single-pass and the first forward-reflected beams will be

$$\rho = \frac{2L \cos(\theta) \sin(\theta)}{\sqrt{n^2 - \sin^2(\theta)}}, \quad (19)$$

where  $L$  is the cavity thickness,  $\theta$  is the tilt angle of the cavity, and  $n$  is the mean refractive index in the cavity. With the collection lens and fiber arranged to efficiently collect the single-pass light (intensity  $I_1$ ), the fractional power in the first reflected beam (intensity  $I_{FR1}$ ) that will be collected is given by (assuming Gaussian beam profiles)

$$\frac{I_{FR1}}{I_1} = R^2 \exp\left(-\frac{2\rho^2}{w^2}\right), \quad (20)$$

where  $R$  is the intensity reflection coefficient and  $w$  is the beam radius (defined by the  $1/e^2$  point). Combining Equations (19) and (20) gives the fractional power ratio between the first reflected beam and the single-pass beam.

In order to minimize ripple in the DGD spectrum, the ratio of Equation (20) should be minimized. To demonstrate the effectiveness of tilting the cavity, we used the same pigtailed wave-

plate geometry measured in Figures 4 and 5 except with the quartz plate tilted by approximately  $4\text{-}5^\circ$  with respect to the incoming beam. For our collimating lenses,  $w = 0.25$  mm,  $L = 9.97$  mm, and  $n = 1.532$ , and we estimate  $R \approx 0.02$ . Equations (19) and (20) indicate that for the given parameters, the first reflected beam will be severely attenuated ( $\sim 150$  dB) from the single-pass beam. Therefore, we expect to see no spectral ripple on the DGD of this device. Figure 7 shows the measured spectrum for the tilted-plate device. Indeed, within the noise of the measurement, no spectral ripple can be seen.

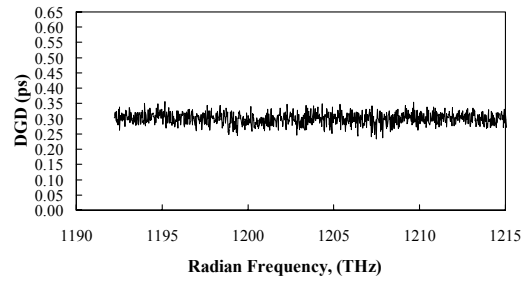


**Figure 7.** Measured DGD spectrum for pigtailed quartz plate with  $4\text{-}5^\circ$  tilt of plate with respect to beam path.

## V. Conclusion

We have characterized the effects on the DGD of a component with multiple reflections present. The resulting DGD spectral ripple has an amplitude proportional to the product of the intensity reflection coefficient and the single-pass group delay of the cavity. We have also shown that tilting a reflective cavity can successfully eliminate the multiple reflection effects on the measured DGD.

## References:

- [1] Normand Cyr, Michel Leclerc and Bernard Ruchet, "PMD measurements in multipath components: The single waveplate example", *Proceedings of Photonics North*, Quebec (2002).
- [2] E. Hecht and A. Zajac, *Optics*, (Addison-Wesley, 1974), p. 305.
- [3] P.A. Williams, "Modulation phase-shift measurement of PMD using only four launched polarization states: a new algorithm," *Electron. Lett.* **35**, 1578-1579 (1999).
- [4] P.A. Williams, "PMD Measurement Techniques – Avoiding Measurement Pitfalls," Presented at the Venice Summer School on PMD, Venice, (2002).